



REVIEW ARTICLE

# A review on recent application of proton transfer photophysics of bipyridine-3,3'-diol in organized assemblies

SOURAV NANDI and NILMONI SARKAR\*

Department of Chemistry, Indian Institute of Technology, Kharagpur, West Bengal 721302, India  
E-mail: nilmoni@chem.iitkgp.ac.in

MS received 17 June 2022; accepted 11 August 2022

**Abstract.** The rich photophysics of the excited-state intramolecular proton transfer (ESIPT) process in 2,2'-Bipyridine-3,3'-diol (BP(OH)<sub>2</sub>) system has interested a lot of researchers from both the experimental and the theoretical sides. The resemblance of BP(OH)<sub>2</sub> with Watson-Crick canonical base pairs of DNA has led to some interesting spectroscopic investigation. Several efforts have been made to arrive at a detailed mechanism of the ESIPT process that generates the “stepwise or concerted?” question, which has been a controversy for years. This controversy led to an enlightening discussion on excited state symmetry and symmetry conservation during the ESIPT process. Under this context, the time has ripened to make a concise view of the fundamental photophysics of this molecule in various organized media, like, micelles, vesicles, fibrils, etc. Moreover, the recent application of this molecule as a fluorescent marker is seen in many self-assembled aggregates formed by various biomolecules, which needs to be highlighted to let the researchers acknowledge it. With this aim, the review, however, by all means, is not an exhaustive article information collection that covers all aspects of ESIPPT, rather, it will mostly focus on the recent application of this probe in many organized assemblies.

**Keywords.** BP(OH)<sub>2</sub>; ESIPT; Photophysics; Vesicles; Fibrils.

## 1. Introduction

In the context of the various chemical and biological processes, a significant amount of interest is there in the excited state intramolecular proton transfer (ESIPT) processes/reactions. This is because of the versatile degree of the extensive application of this ESIPT process in the design of luminescent materials, the formation of the photostabilizers as well as electronic devices, and the construction of proton transfer lasers.<sup>1–7</sup> These proton transfer probes, because of their significant degree of solvatochromism, have found extensive application in determining the nature of the microenvironment of different chemical as well as biological confinements.<sup>8–15</sup> Among the various proton transfer probes reported, one fascinating intramolecularly double hydrogen bonded proton-transfer (PT) probe is Bipyridine-3,3'-diol, BP(OH)<sub>2</sub>, the photophysical behavior of which is significantly altered in response to the alteration of the immediate microenvironments.<sup>16–18</sup> A bimodal degree of the mechanistic insight of this molecule has been reported

for the excited state intramolecular double proton transfer (ESIDPT) sequence, which has been reported to take place as either concerted or the stepwise protocol (Figure 1 a,b).<sup>19–25</sup> In Figure 1b, the associated time scale for the protocol of the direct generation of the diketo form through the abstraction of protons has been mentioned to be in the order of 100 fs.<sup>25</sup> However, according to some other reports, if the process takes place in the two-step mechanism, first, the generation of the monoketo form from the dienol (DE) occurs in the time scale of 50 fs followed by the abstraction of the second proton in the timescale of 10 ps.<sup>25</sup> Not to mention, the transition energy for the S<sub>0</sub> to S<sub>1</sub> for the DE form (Figure 1b) has been reported to be 29100 cm<sup>-1</sup> with a transition dipole moment of 6.27 D.<sup>26</sup> In other words, the explanation in favor of the concerted process of the ESIDPT of BP(OH)<sub>2</sub> reported the femtosecond ordered fast character of the ESIDPT,<sup>24,27–30</sup> whereas the explanation in favor of the sequential mechanistic pathway indicates the formation of the excited state monoketo (MK) tautomer of 100 fs time scale as the prior step and the subsequent relaxation process to the diketo (DK) tautomer

\*For correspondence

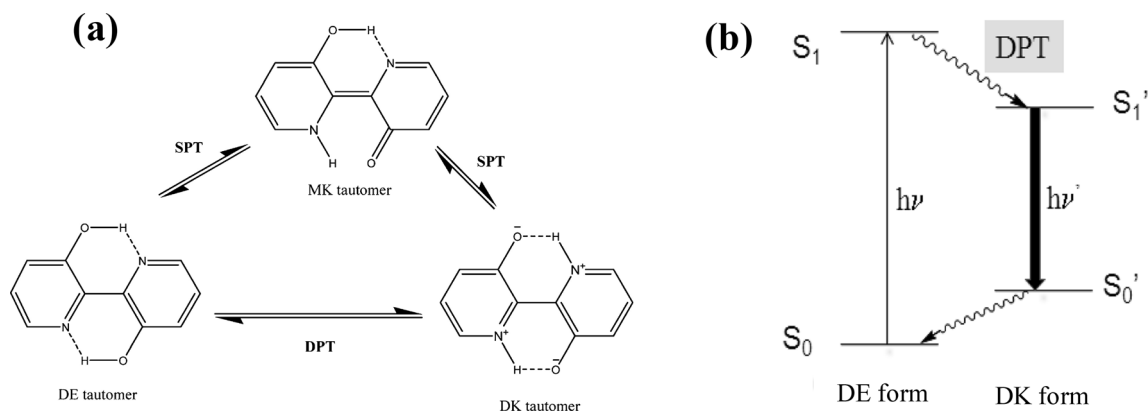


**Figure 1.** (a) Different photo-tautomers involved in the ESIDPT process of BP(OH)<sub>2</sub> showing the step-wise and concerted mechanisms. The image is reproduced with permission from ref. 19 (Copyright 2013 American Chemical Society). (b) Double proton transfer diagram of BP(OH)<sub>2</sub>. The image is reproduced with permission from ref. 25 (Copyright 2013 American Chemical Society).

of emissive character in the timescale of 10 ps in the next step.<sup>19</sup> In this aspect, Zhang *et al.*<sup>27</sup> and Toele *et al.*<sup>28</sup> experimentally comprehended that both the sequential and the concerted path may demand concurrent taking place, which is mostly based on the investigating system along with the excitation and emission wavelengths. Here it is important to mention that, because of the nonpolar characteristics of either of the DE or DK forms, the emission of the probe has been reported to be negligibly altered with the alteration of the solvent polarity.<sup>17,31</sup> However, based on the steady-state and the time-resolved spectroscopic investigation of BP(OH)<sub>2</sub>, Abou-Zied *et al.* reported that the emission maxima of the probe in the protic solvent are shifted to the short wavelength region (blue shift) because of the perturbation of the intramolecular hydrogen bonds.<sup>17</sup> In terms of the absorption spectra of this probe in water, Kundu *et al.* reported a major peak around 340 nm, the signature of the  $\pi-\pi^*$  transition,<sup>32</sup> and the characteristic second band in the region around 400–430 nm.<sup>17</sup> However, both the DE and the DK form of this probe have been reported to have a lower magnitude of the dipole moment, because of which the alteration of the spectral position of either of the absorption or emission spectra are shifted to a less extent in response to the alteration of the solvent polarity.<sup>32</sup> Such altered degree of the spectroscopic signature of this probe molecule has been utilized to unveil the internal property of a number of organized assemblies, like, micelles, vesicles, fibrils, etc. Hence, the versatile application of this probe molecule is worth documenting as a form of review article representation. Briefly, this review article aims to discuss PT reactions in model organic molecules from a spectroscopist's point of view, followed by their application in several biophysical

systems to extract important dynamical information at the subnanosecond time scale. We believe it is central to focus on these processes from a spectroscopic eye as they occur on fast time scales (mostly in the subnanosecond), and their dynamics can be appropriately clocked using short pulses of lasers. The review, however, by all means, is not an exhaustive article that covers all aspects of PT reactions, and hence more detailed references are cited wherever the need is felt for the explanation of things that lie beyond the scope of this article.

## 2. Fundamental photophysics of BP(OH)<sub>2</sub>

The rich photophysics of the excited state intramolecular double proton transfer process (ESIDPT) in BP(OH)<sub>2</sub> system has interested a lot of researchers from both the experimental and the theoretical sides for a long back. The resemblance of BP(OH)<sub>2</sub> with canonical Watson-Crick base pairs in DNA has the underlying motivation for the researchers to study the ESIDPT dynamics of this molecule.<sup>33</sup> In 1983, Bulska reported the first study of cooperative ESIPT in BP(OH)<sub>2</sub> system,<sup>34</sup> where it was shown that the ESIPT emission of BP(OH)<sub>2</sub> was green in nature with a large Stokes shift of 10,000 cm<sup>-1</sup> and a quantum yield of 22% at room temperature. This green photoluminescence was attributed to the radiative relaxation of the excited diketo (DK\*) form.<sup>34</sup> Although later on, studies by Sepiol *et al.*<sup>35</sup> and Langkilde *et al.*<sup>36</sup> show that some population of DK\* relaxes to a dark and relatively long-lived triplet state, thus emphasizing the role of the triplet state in ESIPT process for BP(OH)<sub>2</sub> system. In this aspect, based on the theoretical calculations, Bulska suggested that the driving force for

proton transfer in the excited state of  $\text{BP(OH)}_2$  is probably associated with the increase in electron density over N atoms upon photoexcitation and a parallel decrease in electron density over O atoms of  $\text{BP(OH)}_2$ .<sup>34</sup> The study also hinted that the  $\text{C}_{2h}$  symmetry of the  $\text{BP(OH)}_2$  molecule in the ground state of dienol (DE) form probably favored the formation of the asymmetrical excited state which is only obtainable if a double proton transfer takes place.<sup>37</sup> In 1986, Bulska and co-workers came up with a follow-up study,<sup>38</sup> which was the classic 'OH deletion experiment'. Here a comparison was drawn between ES IPT emission from  $\text{BP(OH)}$  and  $\text{BP(OH)}_2$  by doing temperature resolved fluorescence measurements. A dramatic change in room temperature fluorescence quantum yield of  $\text{BP(OH)}_2$  (quantum yield = 0.22) was observed upon the removal of one OH group from  $\text{BP(OH)}_2$  to form  $\text{BP(OH)}$  (quantum yield = 0.001). Low temperature (77K) fluorescence measurements showed approximately 35 times increase in the fluorescence quantum yield of  $\text{BP(OH)}$ , but even at 77K, the fluorescence quantum yield of  $\text{BP(OH)}_2$  (0.60) was significantly higher than that of  $\text{BP(OH)}$  (0.047). The large Stokes shift in the fluorescence emission of both  $\text{BP(OH)}$  and  $\text{BP(OH)}_2$  was attributed to the ES IPT process. This result was in agreement with the result obtained from INDO/S calculations on the same system.<sup>34</sup> This added further mechanistic support to justify the proposed driving force for proton transfer upon photoexcitation. In 1996 Zhang *et al.* published remarkable experimental observations where they monitored the sub-picosecond dynamics of ES IPT process with the help of femtosecond optical gating (also called fluorescence upconversion) experiments.<sup>27</sup> The main finding of this study was the experimental evidence of a short-lived fluorescence band at 568 nm ( $17606 \text{ cm}^{-1}$  or appx. 17.6 kK) which was assigned to the emission from the keto-enol tautomer, thus elucidating the stepwise proton transfer mechanism in  $\text{BP(OH)}_2$ . Since this 17.6 kK band was short-lived, this supported the speculation that the first proton transfer that converted the DE form to the MK form, was on sub-picosecond time scales. Zhang *et al.* made an important observation that the emission band due to single proton transfer in the model compound  $\text{BP(OH)}$  studied by Bulska *et al.* in their classic 'OH deletion experiment'<sup>38</sup> and the transient band (17.6 kK) recorded by Zhang *et al.*<sup>27</sup> in their femtosecond optical gating studies were roughly coinciding in position. This led them to conclude that the short-lived band was indeed due to an intermediate MK form that was formed upon single proton transfer. This was perhaps the first experimental evidence to capture the

spectroscopic signature of the MK form which required approximately 300 fs time resolution attained by Zhang and co-workers. Before this study, the existence of the MK form was alluded to by Bulska<sup>34</sup> and Borowicz *et al.*<sup>26</sup> through electro-optical measurements. While the study in 1996 by Zhang *et al.* was one of the earliest experimental evidence of the existence of two competing mechanisms of proton transfer – stepwise or concerted, in  $\text{BP(OH)}_2$  system,<sup>27</sup> several efforts have been made to investigate further if one mechanism is preferred over the other. In this aspect, in the conclusion of their optical gating-based study, Zhang *et al.* speculate on the existence of two competing pathways for the proton transfer in  $\text{BP(OH)}_2$ , and they allude to the competitive dynamics of proton transfer in  $\text{BP(OH)}_2$  by imagining a rather complicated multidimensional representation of the excited singlet potential energy surface where the reaction coordinate has contributions from both single and double proton transfer pathways.<sup>27</sup> In 2009, a theoretical study (albeit in the gas phase) by Plasser *et al.*<sup>39</sup> established a preference for the sequential proton transfer mechanism over the concerted double proton transfer mechanism. Both approximate coupled-cluster singles and doubles (RI-CC2) and time-dependent density functional theory (TDDFT) simulations in this study showed the time evolution of the populations of different forms of  $\text{BP(OH)}_2$  has significant contributions from the MK form. This suggests that the role of MK form is important in the early time dynamics for ES IPT in  $\text{BP(OH)}_2$  molecule.

### 3. Application of $\text{BP(OH)}_2$ in organized supramolecular assemblies

The rich photophysics of the  $\text{BP(OH)}_2$  has been meticulously utilized in the investigation of the various physical properties of a number of supramolecular confinements, like, micelles, vesicles, proteins, cyclodextrin systems, and various binary mixtures.<sup>18,19,25,40–47</sup> The use of the  $\text{BP(OH)}_2$  in the cyclodextrin system was mainly to study the inclusion of this probe in various cyclodextrin systems with different binding stoichiometry. For example, the stoichiometric ratio for the binding of the  $\text{BP(OH)}_2$  with the  $\alpha$ -cyclodextrin ( $\alpha$ -CD) has been deduced to be 1:2 based on the binding of the CD system with  $\text{BP(OH)}_2$  using the absorption and emission spectral profile of the probe in this system.<sup>17</sup> In terms of the binding motif, the inclusion of  $\text{BP(OH)}_2$  to the  $\alpha$ -CD system has been reported to be dominated by the van der Waals and the electrostatic interaction, where the

probe inclusion is found to be axial and centered between the two cavities of  $\alpha$ -CD system. However, in terms of the inclusion of this probe in other CD systems, i.e.,  $\beta$ -CD,  $\gamma$ -CD, etc., the absorption as well as the emission profile of BP(OH)<sub>2</sub> is found to be highly sensitive to the cavity size of the CD system along with the altered degree of the hydrophobicity of the CD systems. Specifically, the decrement of the absorption intensity peaks at the region of 400-450 nm is reported along with the red shift of the fluorescence emission spectra of this probe following the successive decrement of the cavity sizes and hence elevated degree of the hydrophobicity of various CD systems.<sup>17</sup> In another dimension of application, De *et al.* investigated the status of the ground state as well as the excited state dynamics of the BP(OH)<sub>2</sub> in the micellar confinement.<sup>25</sup> They reported the binding kinetics and the quantum yield variation of BP(OH)<sub>2</sub> inside the three micellar nanoconfinement formed by distinct charge and neutral surfactants. Additionally, they found a steady rise in the fluorescence quantum yield of BP(OH)<sub>2</sub> in the surfactant solution when the concentration of the solution reached near the critical micellar concentration (CMC), indicating the complete binding of the probe molecules inside the micellar cavity. Again, depending on the nature of the micellar environments which the surfactants provide, the quantum yield was found to be altered (Figure 2a). For example, the maximum quantum yield of BP(OH)<sub>2</sub> was reported in the sodium dodecylsulfate (SDS) solution because of the cationic form of the probes in the region of the Stern layer of the micelle, whereas the increased quantum yield in the neutral Triton X-100 (TX-100) solution arises because of the experience of the probe molecules' maximum hydrophobic microenvironment in the palisade layer of the confinement formed by the TX-100. However, since the micellar confinement formed by the cetyltrimethylammonium bromide (CTAB) provides only a hydrophobic effect, BP(OH)<sub>2</sub> shows the least fluorescence quantum yield among the three micellar confinement studied. Once the micellization process takes place, the enhanced fluorescence quantum yield of the BP(OH)<sub>2</sub> signifies the increased ESIDPT extent experiencing the hydrophobic microenvironment.<sup>25</sup> In another contribution, De *et al.* used BP(OH)<sub>2</sub> as a marker to investigate the structural characteristics of the aggregates formed by the albumin and SDS (protein-surfactant interaction) to explore the effect of this albumin-SDS aggregate on the excited state proton transfer of the probe.<sup>40</sup> They reported an initial competitive character of binding of the SDS with either human serum albumin (HSA) or bovine serum

albumin (BSA) at the high-energy binding region of the proteins. In addition to this, based on the enhanced quantum yield of the BP(OH)<sub>2</sub> in these SDS-albumin aggregates (Figure 2b), they complimented the increased extent of the excited state proton transfer of BP(OH)<sub>2</sub>. In addition to such role of BP(OH)<sub>2</sub> as a probe, the dynamic transformation of supramolecular aggregates has also been identified using BP(OH)<sub>2</sub> as a tracing marker. In this context, the photophysical properties of BP(OH)<sub>2</sub> have been used by Ghosh *et al.* to probe the alteration of the aggregation characteristics of surfactant micelles and vesicles formed by alkyltrimethylammonium bromide (C<sub>n</sub>TAB, n = 12, 14, and 16) and alkyltrimethylammonium bromide/c-cholesterol (C<sub>n</sub>TAB (n = 14 and 16)/cholesterol) at various Q values, where Q indicates the cholesterol-to-surfactant molar ratio (Q = [cholesterol]/[surfactant]).<sup>41</sup> The alteration of the various properties of the BP(OH)<sub>2</sub>, like, rotational anisotropy transient decay timescales and profile (Table 1, Figure 2 c), the steady-state fluorescence emission profile (Figure 3a), and a lifetime of the fluorescence was utilized by them as a marker to trace the micellar to the vesicular structural transformation of the assemblies upon addition of cholesterol (Chol). Here it is important to mention that, at Q=0, no Cholesterol is present in the system, which indicates the neat surfactant solution of either CTAB or TTAB. Since at Q=0, the probe BP(OH)<sub>2</sub> experiences a homogeneous environment, therefore, it shows a single component of a lifetime ( $\tau_2$ ) with its corresponding contribution (a2) (Table 1). However, as Cholesterol was added, the probe BP(OH)<sub>2</sub> experienced multiple locations with different lifetimes that were assigned as  $\tau_1$  and  $\tau_2$  (Table 1). However, the very different constitutional features of a vesicular microenvironment than the micellar environment modulate the ground state as well as the excited state characteristics of BP(OH)<sub>2</sub> to a different extent, the result of which is the different degree of the altered photophysical behavior of the probe molecules in these two distinct supramolecular assemblies, i.e., micelles and vesicles.<sup>41</sup> Again, Iyer *et al.* investigated the photophysics of BP(OH)<sub>2</sub> inside the Nafion membrane confinement and reported the stabilization of both the ground state and the excited state of the BP(OH)<sub>2</sub> in the acidic water content of the Nafion confinement.<sup>42</sup> The surprising fact they reported in this contribution indicates the presence of the dianionic enolate form in its excited state (Figure 3b) inside the Nafion confinement under acidic conditions, which is usually present in the neat alkaline aqueous solution. In other contributions, Satpathi *et al.* investigated a comparative study on the ESIDPT dynamics of the

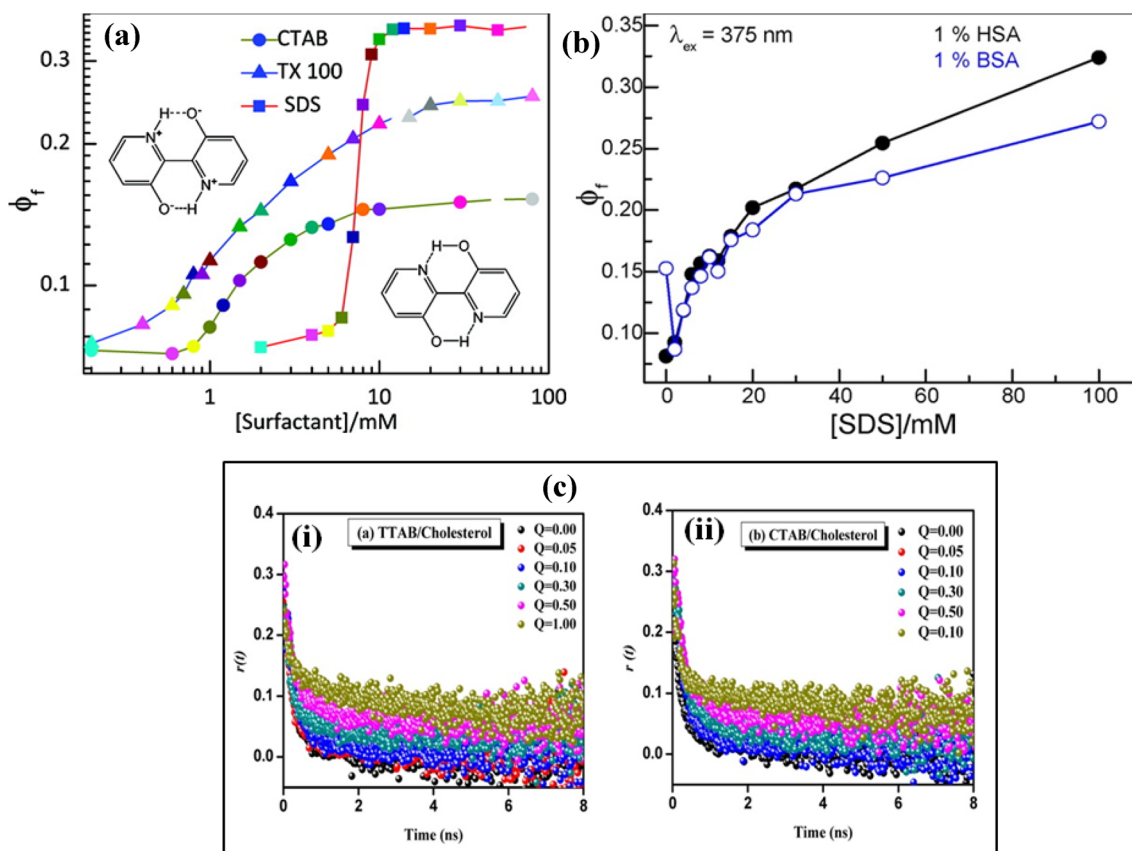


**Figure 2.** (a) Fluorescence quantum yield plots of BP(OH)<sub>2</sub> in aqueous solution with increasing concentration of the surfactants, CTAB, TX-100, and SDS.  $\lambda_{ex} = 350$  nm. (b) Quantum yield of BP(OH)<sub>2</sub> in 1% HSA and 1% BSA as a function of SDS concentration from 0 to 100 mM. ( $\lambda_{ex} = 375$  nm.) (c) Anisotropy decays of BP(OH)<sub>2</sub> in water and 30 mM (i) TTAB and (ii) CTAB solutions with increasing cholesterol concentration ( $\lambda_{ex} = 375$  nm). Image (a) is reproduced with permission from ref. 25 (Copyright 2011 American Chemical Society); Image (b) is reproduced with permission from ref. 43 (Copyright 2012 American Chemical Society); Image (c) is reproduced with permission from ref. 44 (Copyright 2014 American Chemical Society).

**Table 1.** Time-Resolved Fluorescence Decay Parameters of BP(OH)<sub>2</sub> in Surfactant/Cholesterol System at Different Q Values ( $\lambda_{ext} = 336$  nm), where  $Q = [\text{cholesterol}]/[\text{surfactant}]$ .<sup>41</sup> The information is reproduced with permission from ref. 44 (Copyright 2014 American Chemical Society).

System	Q value	$\tau_1$ (ns)	$a_1$	$\tau_2$ (ns)	$a_2$
Cholesterol/TTAB	0	—	—	1.90	1.00
	0.05	1.38	0.26	2.15	0.74
	0.10	1.65	0.60	2.53	0.40
	0.30	1.79	0.66	3.15	0.34
	0.50	1.84	0.51	3.34	0.49
	1.00	1.91	0.61	3.42	0.39
Cholesterol/CTAB	0	—	—	2.08	1.00
	0.05	1.63	0.20	2.24	0.80
	0.10	1.67	0.36	2.37	0.64
	0.30	1.81	0.61	2.96	0.39
	0.50	1.82	0.53	3.21	0.47
	1.00	1.85	0.50	3.24	0.50

BP(OH)<sub>2</sub> in a number of micellar confinement, like, octyl- $\beta$ -D-glucoside (OBG) micelle, SDS micelle, and CTAB micelle.<sup>43</sup> An altered degree of the proton transfer time scales were reported by them in these assemblies, which range between 11 to 30 ps, where the origin of these altered time scales in the various supramolecular assemblies studied has been concluded to be due to variable degree of the water accessibility of the probe molecules. Specifically, inside the OBG micellar confinement, the absorption spectra of BP(OH)<sub>2</sub> (Figure 3c) show the ground state conversion from DK to DE. Again, the resulting fluorescence upconversion traces (Figure 3d) estimates a time scale of 13 ps for the ESIDPT process of the BP(OH)<sub>2</sub> inside the OBG micellar confinement, thereby indicating the sequential ESIDPT protocol inside this environment. However, inside the anionic SDS micellar environment, the ESIDPT dynamics timescales were

estimated to be 30 ps. They proposed that the origin of these altered time scales of ESIDPT dynamics of  $\text{BP}(\text{OH})_2$  in the various supramolecular assemblies is the result of the variable degree of the water accessibility of the probe molecules.<sup>43</sup>

The altering degree of the binding dynamics of the  $\text{BP}(\text{OH})_2$  has been utilized to understand its binding chemistry with a number of bile salt aggregates having varying degrees of hydrophobicity. This becomes possible because of the appreciable change in the ground state as well as the excited state binding dynamics of  $\text{BP}(\text{OH})_2$ , which is extremely sensitive to the structural alterations of the bile salts. For example, the absorption spectra of the probe were recorded by Sarkar *et al.* and reported that the value of the absorbance was increased at 340 nm in the presence of the bile salts (Figure 4a i,ii,iii).<sup>16</sup> This addition of the bile salts results in the decrement of the absorbance at the region of the wavelength of 400 to 450 nm (Figure 4a i,ii,iii). The increased absorbance value at 340 nm in

the presence of the added bile salts is a signature of the formation of host-guest inclusion complexes. Not to mention, in these absorption plots (Figure 4a i,ii,iii), the absence of the isosbestic points indicates that no simple two-state equilibrium is there,<sup>25</sup> which simply concludes the variable degree of binding of the probes to the different binding sites of the bile salt aggregates. In the case of the fluorescence emission spectra of the probe (Figure 4b i,ii,iii), it was reported the increased emission intensity as well as the red shifting of the emission maxima in the presence of the increased concentrations of the bile salts, which has been ascribed to be associated with the incorporation of the probes inside the hydrophobic region of the bile salt aggregates, an alike binding signature of the probes in the cyclodextrin system.<sup>17,31</sup> However, in terms of the extent of the red-shifting of the emission maxima (Figure 4b), it was prominent in the case of the sodium deoxycholate (NaDC) compared to the sodium cholate (NaCh) and sodium taurocholate (NaTc), which

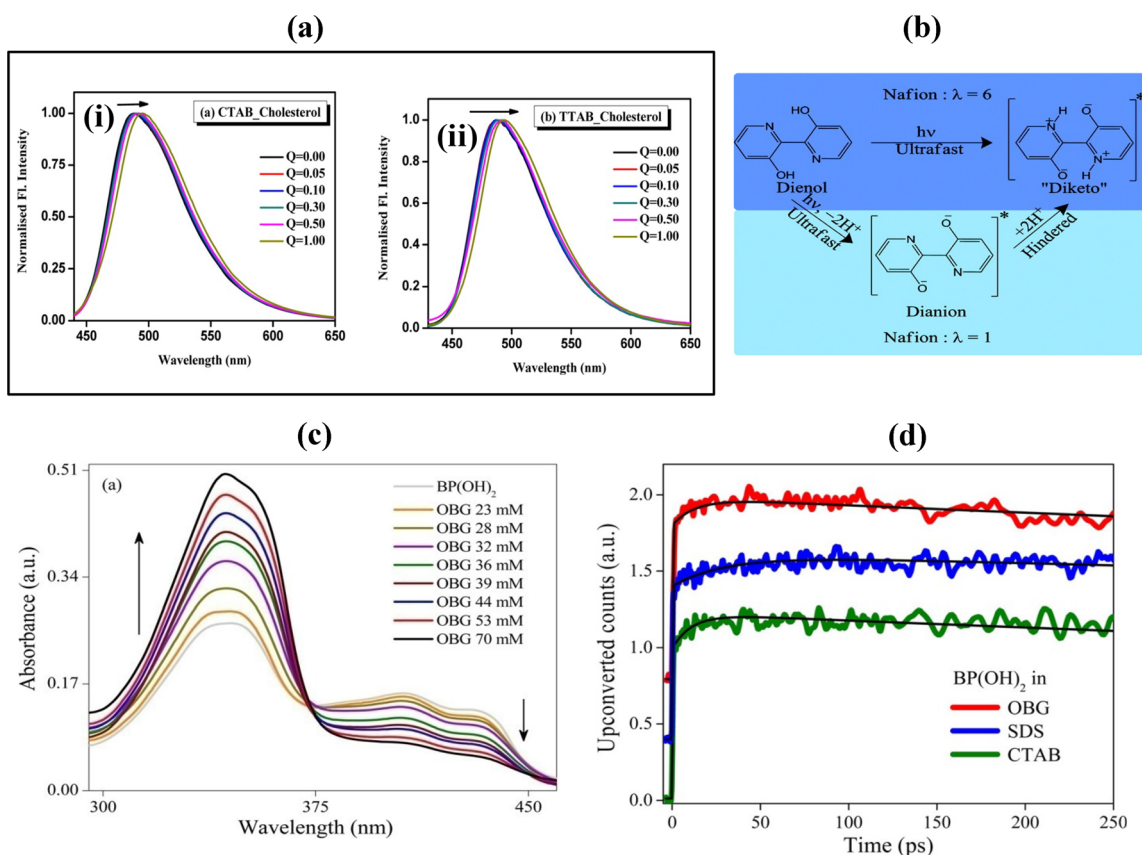


**Figure 3.** (a) Steady state fluorescence spectra of  $\text{BP}(\text{OH})_2$  in 30 mM (i) CTAB and (ii) TTAB with an increase in cholesterol concentration. (b) Concerted ESIDPT of  $\text{BP}(\text{OH})_2$  in Hydrated Nafion and Excited State Double Deprotonation in the Dehydrated Membrane. (c) Absorption spectra of  $\text{BP}(\text{OH})_2$  (10  $\mu\text{M}$ ) in presence of 0 to 70 mM of OBG surfactants. Arrow indicates the direction of increasing OBG concentration. (d) Fluorescence up-converted decay profiles of  $\text{BP}(\text{OH})_2$  in different micellar environments. Decay profiles ( $\lambda_{\text{ex}} = 375 \text{ nm}$ ) are collected at emission maxima. Best fits are shown as black colored line. Image (a) is reproduced with permission from ref. 44 (Copyright 2014 American Chemical Society); Image (b) is reproduced with permission from ref. 45 (Copyright 2012 American Chemical Society); Images (c), (d) are reproduced with permission from ref. 46 (Copyright 2015 American Chemical Society).

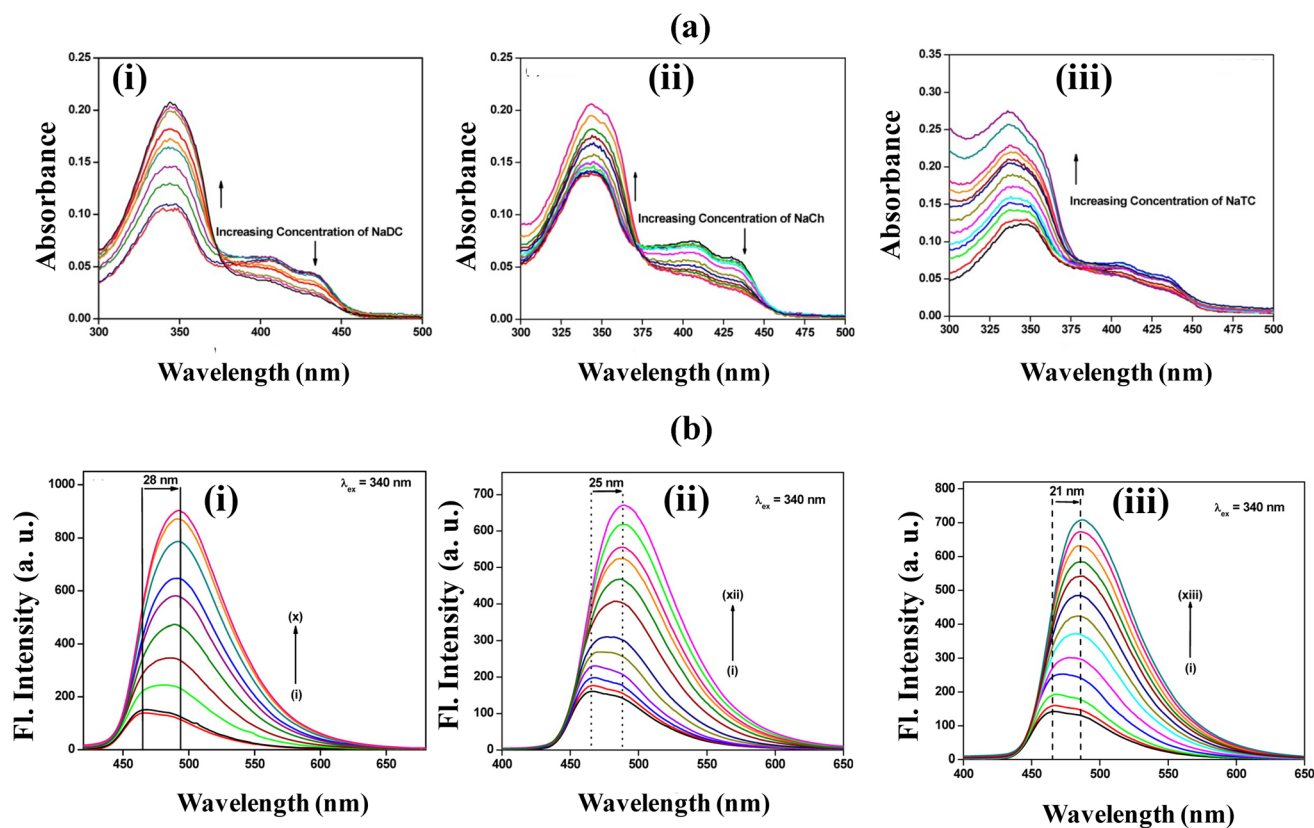


**Figure 4.** (a) UV–vis absorption spectra of BP(OH)<sub>2</sub> in aqueous 0.2 M NaCl solution with increasing concentration of (i) NaDC (0–40 mM), (ii) NaCh (0–40 mM), and (iii) NaTC (0–40 mM). (b) Steady-state fluorescence spectra ( $\lambda_{\text{ex}} = 340$  nm) of BP(OH)<sub>2</sub> in aqueous 0.2 M NaCl solution with increasing concentration of (i) NaDC (curves i–x correspond to 0–40 mM NaDC), (ii) NaCh (curves i–xii correspond to 0–40 mM NaCh), and (iii) NaTC (curves i–xiii correspond to 0–40 mM NaTC). These images are reproduced with permission from ref. 16 (Copyright 2013 American Chemical Society).

indicates the presence of a more hydrophobic environment in case of the NaDC compared to the other two bile salt aggregates. Hence, the spectroscopic absorption and the emission signature of probe BP(OH)<sub>2</sub> marks the extent of the hydrophobic effect on the properties of the aggregates formed by the bile salts.

In terms of other advanced applications, the signature of the modulation of the ESIDPT of BP(OH)<sub>2</sub> in the crown ether systems (18-Crown-6, 18C6 and 15-Crown-5, 15C5) is worth explaining the behavior of the probe with special attention towards the application of the probe in the sensing of the fibrillar morphologies form by the amino acids. Considering this, Banik *et al.*<sup>48</sup> found the absence of significant interaction between the BP(OH)<sub>2</sub> and the crown ethers, as mentioned, based on the UV-visible spectra (Figure 5a i,ii). However, an interesting feature was observed in the fluorescence emission study of the probes in the crown ether system, which includes the presence of an additional emission band at ~ 415 nm along with the emission band corresponding to the

diketo tautomer band at ~ 465 nm (Figure 5b i,ii). In the time-resolved fluorescence emission studies (Figure 6 a-d), they found the presence of a rise component of magnitude ~ 260 ps in the 18C6 system (Figure 6c), which was absent in the 15C5 system. They have proposed that the water-assisted ESIDPT protocol of the probe actually forms H<sub>3</sub>O<sup>+</sup> species at the excited state with which 18C6 can preferably bind,<sup>49,50</sup> the result of which is the decreased ESIDPT dynamics.<sup>48</sup> However, for 15C5, because of the inability to bind with the H<sub>3</sub>O<sup>+</sup>, no rise component was found.

On the other hand, the probe BP(OH)<sub>2</sub> has found its application in the amyloid field of research, where amyloid-like fibrillar aggregates are being characterized using this probe. Identifying these fibrillar morphologies is extremely important from the therapeutic point of view since such fibrillar aggregates have been reported to be toxic.<sup>51,52</sup> In this aspect, the study by Perween *et al.*<sup>53</sup> has reported the formation of the glycine fibrils, which was characterized with the help of staining with a conventional fibril marker

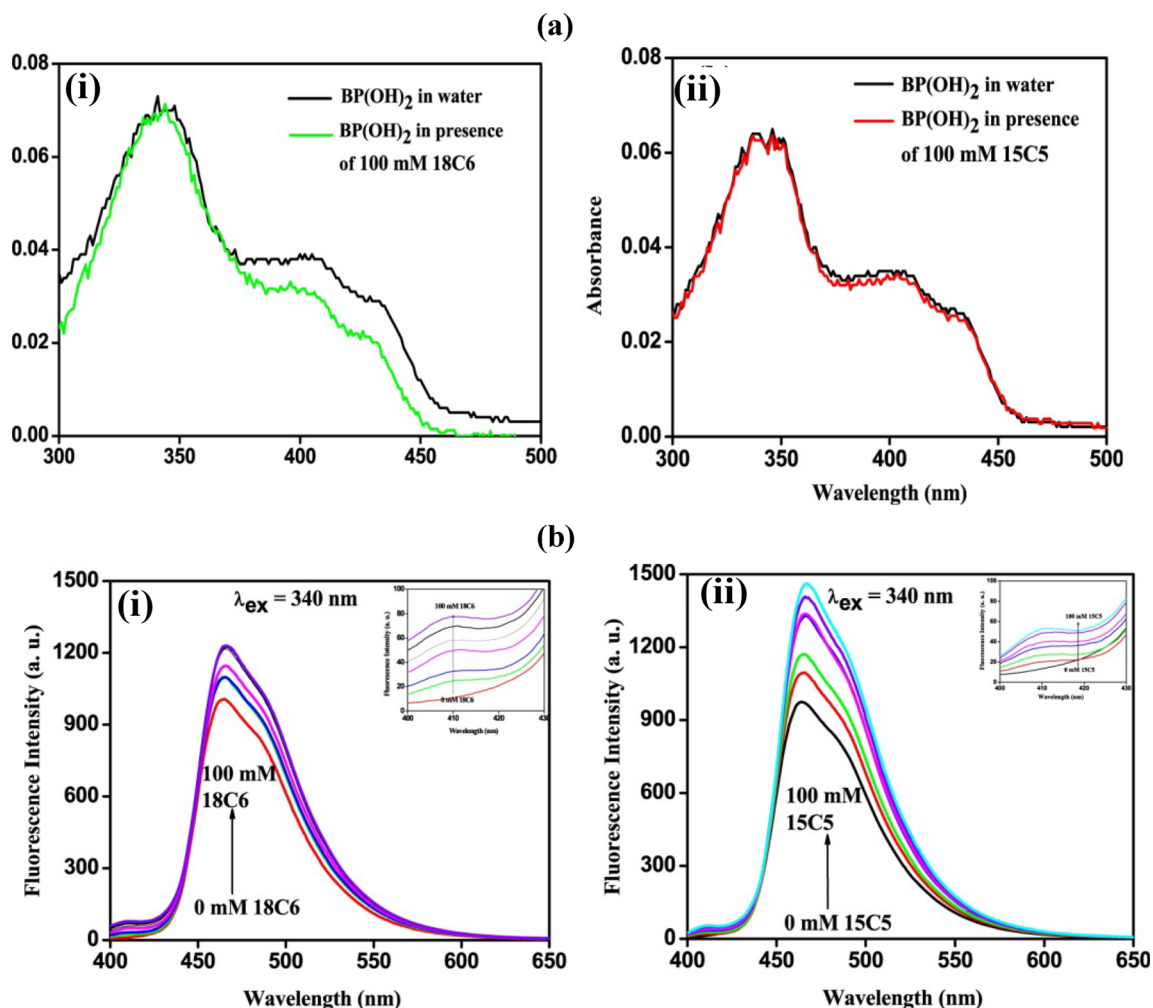


**Figure 5.** (i) Steady-state UV–vis absorption spectra of BP(OH)<sub>2</sub> in crown ether concentrations of 0 and 100 mM: (a) 18-Crown-6 (b) 15-Crown-5. (ii) Steady-state fluorescence spectra of BP(OH)<sub>2</sub> as a function of increasing CE concentration (0–100 mM): (a) 18-Crown-6 and (b) 15-Crown-5. (Inset shows the appearance of the 415 nm band as a function of CE concentration.) These images are reproduced with permission from ref. 53 (Copyright 2016 American Chemical Society).

fluorophore thioflavin T (ThT) (Figure 7a). Although the enormous increase in the intensity of ThT in the samples proves the formation of amyloid-like fibrillar structures,<sup>54,55</sup> still a great deal of debate is in the literature regarding the justification of using this probe as a fibril sensor exclusively. For example, Sulatskaya *et al.* reported that the signature of the enhanced emission intensity of the ThT might not be associated exclusively with the incorporation of the probes inside the fibrillar etiology but also may originate from the formation of the excimer in highly concentrated aqueous solutions.<sup>56</sup> This apparent anomaly of the fibril sensing nature of the ThT was overcome by researchers<sup>48</sup> through their work using BP(OH)<sub>2</sub> as a fibril sensor, as observed in the case of the fluorescence lifetime imaging microscopy (FLIM) investigation of the glycine fibril (Figure 7b i, ii, 7c i–iv, 7d). Fluorescence Lifetime Imaging Microscopy

(FLIM) is a well-known microscopic technique that provides the opportunity to record the image-based information for various macromolecular aggregates as well as the binding, conformation, and composition of biologically relevant compounds.<sup>48,52,57,58</sup> Using this technique, BP(OH)<sub>2</sub> has been reported to be successfully applied for the sensing of the neat glycine fibrils (Figure 7b i,ii), as well as the fibrillar etiology in the presence of 18C6 (Figure 7c i,ii) and 15C5 (Figure 7c iii,iv).<sup>48</sup> In addition to the image-based visualized etiology information, the lifetime of the BP(OH)<sub>2</sub> was also mentioned to be considerably different to indicate the different etiologies of the glycine fibrils in the presence of 18C6 and 15C5 (Figure 7d).

The dynamic transformation of supramolecular aggregates has also been identified using BP(OH)<sub>2</sub> as a tracing marker.<sup>41</sup> In 2014, Ghosh *et al.* studied the micelle to vesicle transition induced by cholesterol

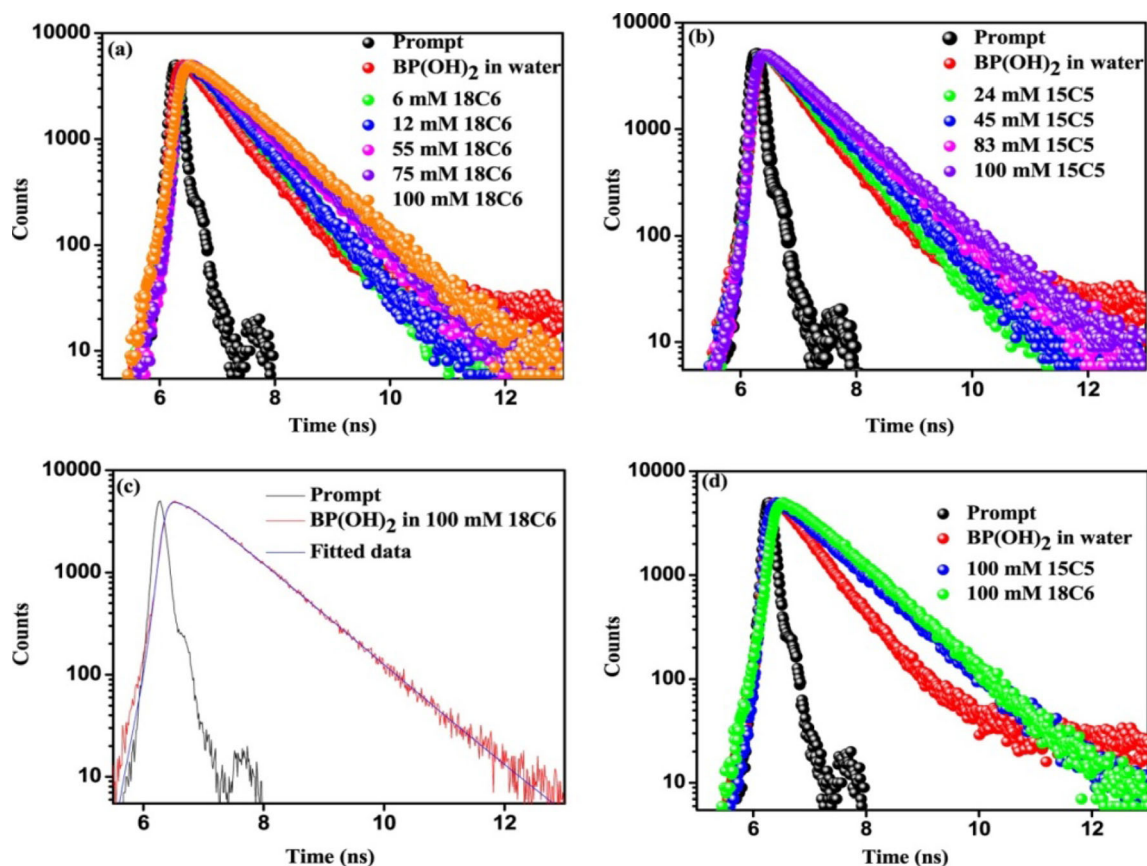


**Figure 6.** Time-resolved fluorescence decays of  $\text{BP(OH)}_2$  with increasing concentrations of (a) 18C6 and (b) 15C5. (c) Time-resolved rise of  $\text{BP(OH)}_2$  in the presence of 100 mM 18C6. (d) Comparison of  $\text{BP(OH)}_2$  in 100 mM 18C6 and 15C5. These images are reproduced with permission from ref. 53 (Copyright 2016 American Chemical Society).

addition, using  $\text{BP(OH)}_2$  as a fluorescent probe.<sup>41</sup> From steady-state absorption measurements, it was found that an increase in surfactant concentration led to a hypochromic shift for the absorption band in the 400–450 nm region, whereas a hyperchromic shift was observed for the absorption band in the 340 nm region. This was explained by suggesting that in the presence of surfactants, the  $\text{BP(OH)}_2$  molecules were incorporated into the hydrophobic micelle which leads to stabilization of the DE form that results in the increase in absorbance near the 340 nm region. The hypochromic feature in the steady-state absorption was explained by the reduction of hydrogen bonding interaction between water molecules and the DK form in the ground state because of the incorporation of the  $\text{BP(OH)}_2$  molecules in the hydrophobic region of the micelle.<sup>41</sup> A potential application of this effect could be the use of DK absorption band of  $\text{BP(OH)}_2$  as a sensor of water in surfactant assemblies.<sup>41</sup> This was also nicely supported by a detailed solvent effect study of the steady-state absorption and fluorescence spectra of  $\text{BP(OH)}_2$ , as reported by Abu-Zied,<sup>33</sup> where no measurable solvatochromic effect in the steady-state

absorption of  $\text{BP(OH)}_2$  was observed. This was attributed to the low ground state dipole moment of the DE tautomer (major form). However, an additional structure close to 450 nm was found in the steady-state absorption spectrum when the solvent was water. This was absent in any other solvent, including a polar protic solvent like MeOH, and thus it was proposed that this feature arises due to the high tendency of water molecules to form hydrogen bonds. In the case of the effect of micellar confinement on the steady-state fluorescence spectra of  $\text{BP(OH)}_2$ , a hyperchromic shift was there, as expected.<sup>41</sup> This is because incorporation of  $\text{BP(OH)}_2$  molecules in the hydrophobic region of micelle provides stabilization and slows down the rates of nonradiative relaxation, thereby making the decay through the fluorescence channel more predominant. This was also quantitatively mapped out through concentration-dependent measurements. Upon addition of cholesterol, it was found that there occurs a micelle to vesicle transition. Based on steady-state and time-resolved measurements, Ghosh *et al.*<sup>41</sup> found that  $\text{BP(OH)}_2$  preferably located itself in the bilayer of the vesicle. This was supported by the

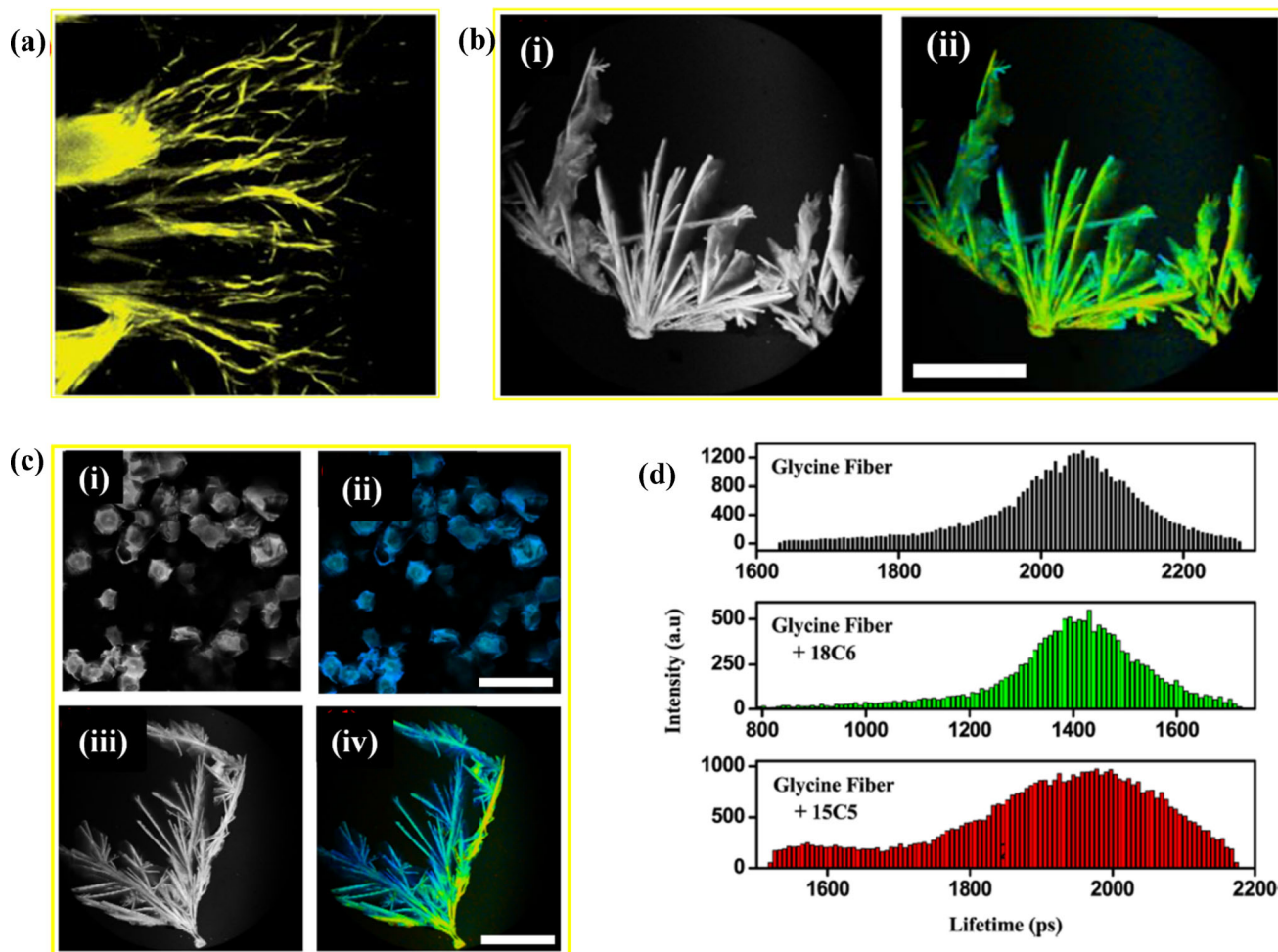


**Figure 7.** (a) Fibres observed at the edge of the microscope slide of ThT + Glycine. (b) (i) Fluorescence intensity and (ii) lifetime images of the glycine fibril. (Scale bar is 25  $\mu\text{m}$ .) (c) Modulation of the fiber morphology of glycine in the presence of 18C6 (i, ii) and 15C5 (iii, iv). [Fluorescence intensity images: (i) and (iii), lifetime images: (ii) and (iv).] (Scale bar is 25  $\mu\text{m}$ .) (d) Lifetime distribution of BP(OH)<sub>2</sub> inside the glycine fibril and in the presence of 18C6 and 15C5. (a) The image is reproduced with permission from ref. 58 (Copyright 2013 RSC). (b, c, d) These images are reproduced with permission from ref. 53 (Copyright 2016 American Chemical Society).

studies in the micellar system, where it placed itself in the hydrophobic part of the micelles.<sup>41</sup> Furthermore, fluorescence anisotropy measurements suggested an increase in microviscosity inside the vesicular bilayer, which was corroborated by the slowing down of the rotational dynamics.<sup>41</sup> This study showed how BP(OH)<sub>2</sub> can be used to probe hydrophobic environments, thus suggesting the potential use of this molecule's ground and excited state spectroscopic signatures to study several other host-guest interactions.<sup>41</sup>

#### 4. Future perspectives

One of the promising applications that can still be expanded for this molecule is the application as a fluorescent marker for amyloid aggregates. As

mentioned in the discussion, it is seen that the fluorescence signal of this molecule can be used to track the formation of the fibrillar structure formation by the natural amino acid Glycine. The formation of the amyloid fibrillar aggregates by the natural amino acids having aromatic moieties in their structure is very common that is usually recorded using the fluorescence signal of the probe thioflavin T (ThT).<sup>59,60</sup> However, because of the complicated photophysics of the thioflavin T, researchers have recommended its limited use for the detection of the amyloid aggregates formed by the biomolecules.<sup>61–64</sup> Under this context, the application of the BP(OH)<sub>2</sub> can be thought of as the replacement of thioflavin T to investigate the formation and structural aspects of amyloids formed by amino acids and alike molecules. Additionally, since the photophysics of BP(OH)<sub>2</sub> is known to track the

structural transition from one supramolecular confined morphology to others,<sup>41</sup> designs of directed nanoarchitectures can be done based on the photophysical behavior of this probe molecule in the designed structure.

On the other hand, in neurological disorders, the contributions of the unprocessed amino acids capable of forming fibrillar morphologies are known to be responsible.<sup>51</sup> To understand the molecular level pathogenesis of such disorders, researchers have synthesized the artificial phospholipid vesicle membrane, the mimicking setup of the cell membrane,<sup>65,66</sup> and investigated the effect of such self-assembled fibrillar morphologies formed by amino acids and their derivatives on the lipid membrane.<sup>67,68</sup> Since BP(OH)<sub>2</sub> is known to mark the vesicle bilayer,<sup>41</sup> the alteration of the properties of the vesicle membrane probed by the toxic fibrillar etiologies formed by amino acids and their derivatives can be investigated using the spectroscopic signature of BP(OH)<sub>2</sub>.

## 5. Conclusions

The present contribution aims to document the application of the fundamental photophysics of the ancient and spectroscopically important molecule BP(OH)<sub>2</sub>. The time scales of the proton transfer dynamics of this molecule, either in the stepwise or concerted pathway, have been reviewed based on the documented literature reports. Additionally, how the spectroscopic signature of this molecule has been used to study the internal organization of several supramolecular confinements, like, micelles, vesicles, proteins, cyclodextrin systems, and various binary mixtures, has been taken into due consideration in this review. In addition to this, how the transition from one supramolecular confined structure to another confined structure by the surfactant molecules takes place, is successfully tracked by the spectroscopic signature of the BP(OH)<sub>2</sub>. The time-resolved rotational anisotropy study using this probe molecule BP(OH)<sub>2</sub> was found to be applied for the investigation of the guest-host interaction in the micelle or the vesicle system. Moreover, the application of this probe molecule as a marker for the amino acid aggregates is expected to broaden the opportunity to use this molecule as an amyloid marker. Taken together, although the photophysical aspects of the proton transfer in the BP(OH)<sub>2</sub> is an old topic, however, the application of its spectroscopic signature to track the various dynamical processes in several biologically important

supramolecular assemblies justifies the urge to present the current review on the given topic.

## Acknowledgements

N. S. gratefully acknowledges the Science and Engineering Research Board (SERB), Council of Scientific and Industrial Research (CSIR), Government of India, and DSTBT, Government of West Bengal, for providing generous research grants. N.S. wishes to thank all M.Sc. and Ph.D. students in his group who contributed to the discussed works.

## References

1. Zhong D, Douhal A and Zewail A H 2000 Femtosecond Studies of Protein–Ligand Hydrophobic Binding and Dynamics: Human Serum Albumin *Proc. Natl. Acad. Sci. U.S.A.* **97** 14056
2. Chattoraj M, King B A, Bublitz G U and Boxer S G 1996 Ultra-fast Excited State Dynamics in Green Fluorescent Protein: Multiple States and Proton Transfer *Proc. Natl. Acad. Sci. U.S.A.* **93** 8362
3. Mueller A, Diemann E, Ratajczak H and Junge W (Ed.) 1992 *Electron and proton transfer in chemistry and biology* (Netherlands: Elsevier)
4. Service R F 2005 Organic LEDs Look Forward to a Bright *White Future Science* **310** 1762
5. Haddon R C and Stillinger F H 1987 In *Molecular Electronic Devices* F L Carter (Ed.) (New York: Marcel Dekker)
6. Park S, Kwon J E, Kim S H, Chung Seo J and K, Park S Y, Jang D J, Medina B M, Gierschner J and Park S Y, 2009 A White-Light-Emitting Molecule: Frustrated Energy Transfer between Constituent Emitting Centers *J. Am. Chem. Soc.* **131** 14043
7. Tang K C, Chang M J, Lin T Y, Pan H A, Fang T C, Chen K Y, et al. 2011 Fine Tuning the Energetics of Excited-State Intramolecular Proton Transfer (ESIPT): White Light Generation in A Single ESIPT System *J. Am. Chem. Soc.* **133** 17738
8. Bhattacharyya K 2003 Solvation Dynamics and Proton Transfer in Supramolecular Assemblies *Acc. Chem. Res.* **36** 95
9. Mandal T, Ghosh S, Das A K, Mandal A K and Bhattacharyya K 2012 Salt Effect on the Ultrafast Proton Transfer in Niosome *J. Phys. Chem. B* **116** 8105
10. Cohen B, Alvarez M, Carmona N, Organero J A and Douhal, 2011 A Proton-Transfer Reaction Dynamics within the Human Serum Albumin Protein *J. Phys. Chem. B* **115** 7637
11. Douhal A 2004 Breaking, Making, and Twisting of Chemical Bonds in Gas, Liquid, and Nanocavities *Acc. Chem. Res.* **37** 349
12. Adhikary R, Carlson P J, Kee T W and Petrich J W 2010 Excited-State Intramolecular Hydrogen Atom Transfer of Curcumin in Surfactant Micelles *J. Phys. Chem. B* **114** 2997
13. Douhal A, Kim S K and Zewail A H 1995 Femtosecond Molecular Dynamics of Tautomerization in Model Base Pairs *Nature* **378** 260

14. Sytnik A, Gormin D and Kasha M 1994 Interplay Between Excited-State Intramolecular Proton Transfer and Charge Transfer in Flavonols and Their Use as Protein-Binding-Site Fluorescence Probes *Proc. Natl. Acad. Sci. U.S.A.* **91** 11968
15. Sytnik A and Litvinyuk I 1996 Energy Transfer to a Proton-Transfer Fluorescence Probe: Tryptophan to a Flavonol in Human Serum Albumin *Proc. Natl. Acad. Sci. U.S.A.* **93** 12959
16. Mandal S, Ghosh S, Aggala H H, Banerjee C, Rao V G and Sarkar N 2013 Modulation of the Photophysical Properties of 2,2'-Bipyridine-3,3'- diol inside Bile Salt Aggregates: A Fluorescence-based Study for the Molecular Recognition of Bile Salts *Langmuir* **29** 133
17. Abou-Zied O K 2010 Steady-State and Time-Resolved Spectroscopy of 2,2'-Bipyridine-3,3'-diol in Solvents and Cyclodextrins: Polarity and Nanoconfinement Effects on Tautomerization *J. Phys. Chem. B* **114** 1069
18. Mandal S, Ghosh S, Aggala H H K, Banerjee C, Rao V G and Sarkar N 2013 Modulation of the Photophysical Properties of 2,2'- Bipyridine-3,3'-diol inside Bile Salt Aggregates: A Fluorescence Based Study for the Molecular Recognition of Bile Salts *Langmuir* **29** 133
19. Mandal S, Ghosh S, Banerjee C, Kuchlyan J and Sarkar S 2013 Unique Photophysical Behavior of 2,2'-Bipyridine-3,3'-diol in DMSO–Water Binary Mixtures: Potential Application for Fluorescence Sensing of  $Zn^{2+}$  Based on the Inhibition of Excited-State Intramolecular Double Proton Transfer *J. Phys. Chem. B* **117** 12212
20. Sepiol J, Grabowska A, Bulska H, Mordzinski A, Perez Salgado F and Rettschnick R P H 1989 The Role of the Triplet State in Depopulation of the Electronically Excited Proton-Transferring System [2,2'-bipyridyl]-3,3'-diol *Chem. Phys. Lett.* **163** 443
21. Barone V, Palma A and Sanna N 2003 Toward a Reliable Computational Support to the Spectroscopic Characterization of Excited State Intramolecular Proton Transfer: [2,2'-bipyridine]-3,3'- diol as a Test Case *Chem. Phys. Lett.* **381** 451
22. Gelabert R, Moreno M and Lluch J M 2004 Quantum Dynamics Study of the Excited-State Double-Proton Transfer in 2,2'-bipyridyl- 3,3'-diol *Chem. Phys. Chem.* **5** 1372
23. Plasser F, Barbatti M, Aquino A J A and Lischka H 2009 Excited-State Diproton Transfer in [2,2'-Bipyridyl]-3,3'-diol: the Mechanism Is Sequential Not Concerted *J. Phys. Chem. A* **113** 8490
24. Marks D, Proposito P, Zhang H and Glasbeek M 1998 Femtosecond Laser Selective Intramolecular Double-Proton transfer in 2,2'-Bipyridyl-3,3' -diol *Chem. Phys. Lett.* **289** 535
25. De D and Datta A 2011 Modulation of Ground- and Excited-State Dynamics of [2,2'-Bipyridyl]-3,3'-diol by Micelles *J. Phys. Chem. B* **115** 1032
26. Borowicz P, Grabowska A, Wortmann R and Liptay W 1992 Tautomerization in Fluorescent States of Bipyridyl-Diols: A Direct Confirmation of the Intramolecular Double Proton Transfer by Electro-Optical Emission Measurements *J. Lumin.* **52** 265
27. Zhang H, van der Meulen P and Glasbeek M 1996 Ultrafast Single and Double Proton Transfer in Photo- Excited [2,2'-Bipyridyl]-3,3'- diol *Chem. Phys. Lett.* **253** 97
28. Toele P, Zhang H and Glasbeek M 2002 Femtosecond Fluorescence Anisotropy Studies of Excited-State Intramolecular Double-Proton Transfer in [2,2'-bipyridyl]-3,3'-diol in Solution *J. Phys. Chem. A* **106** 3651
29. Proposito P, Marks D, Zhang H and Glasbeek M 1998 Femtosecond Double Proton-Transfer Dynamics in [2,2'-bipyridyl]-3,3'-diol in Sol–Gel Glasses *J. Phys. Chem. A* **102** 8894
30. Neuwahl F V R, Foggi P and Brown R G 2000 Sub-Picosecond and Picosecond Dynamics in the S1 state of [2,2'-Bipyridyl]-3,3'-diol Investigated by UV–visible Transient Absorption Spectroscopy *Chem. Phys. Lett.* **319** 157
31. Marks D, Zhang H, Glasbeek M, Borowicz P and Grabowska A 1997 Solvent Dependence of (Sub)Picosecond Proton Transfer in Photo- Excited [2,2'-Bipyridyl]-3,3'-diol *Chem. Phys. Lett.* **275** 370
32. Kundu N, Banerjee P, Dutta R, Kundu S, Saini R K, Halder M and Sarkar N 2016 Proton Transfer Pathways of 2,2'-Bipyridine-3,3'-diol in pH Responsive Fatty Acid Self-Assemblies: Multiwavelength Fluorescence Lifetime Imaging in a Single Vesicle *Langmuir* **32** 13284
33. Abou-Zied O K 2006 Examining [2, 2'-bipyridyl]-3, 3'- diol as a Possible DNA Model Base Pair *J. Photochem. Photobiol. A: Chem.* **182** 192
34. Bulska H 1983 Intramolecular Cooperative Double Proton Transfer in [2, 2'-bipyridyl]-3, 3'-diol *Chem. Phys. Lett.* **98** 398
35. Sepiol J, Grabowska A, Bulska H, Mordziński A, Perez Salgado F and Rettschnick R P H 1989 The Role of the Triplet State in Depopulation of the Electronically Excited Proton-Transferring System [2, 2'-bipyridyl]-3, 3'-diol” *Chem. Phys. Lett.* **163** 443
36. Langkilde F W, Mordzinski A and Wilbrandt R 1992 Time-Resolved Resonance Raman Study of Proton Transferring Systems in the Excited Triplet State: 2, 2'- Bipyridine and 2, 2'-Bipyridine-3, 3'-Diol *Chem. Phys. Lett.* **190** 305
37. Serdiuk I E and Roshal A D 2017 Exploring Double Proton Transfer: A Review on Photochemical Features of Compounds with Two Proton-Transfer Sites *Dyes Pigm.* **138** 223
38. Bulska H, Grabowska A and Grabowski Z R 1986 Single and Double Proton Transfer in Excited Hydroxy Derivatives of Bipyridyl *J. Lumin.* **35** 189
39. Plasser F, Barbatti M, Aquino A J A and Lischka H 2009 Excited-State Diproton Transfer in [2, 2'-Bipyridyl]-3, 3'-Diol: The Mechanism is Sequential Not Concerted *J. Phys. Chem. A* **113** 8490
40. De D, Santra K and Datta A 2012 Prototropism of [2,2'-Bipyridyl]- 3,3'-diol in Albumin–SDS Aggregates *J. Phys. Chem. B* **116** 11466
41. Ghosh S, Kuchlyan J, Roychowdhury S, Banik D, Kundu N, Roy A and Sarkar N 2014 Unique Influence of Cholesterol on Modifying the Aggregation Behavior of Surfactant Assemblies: Investigation of Photophysical and Dynamical Properties of 2,2'-Bipyridine-3,3'-diol, BP(OH)2 in Surfactant Micelles, and Surfactant/

- Cholesterol Forming Vesicles *J. Phys. Chem. B* **118** 9329
42. Iyer E S S and Datta A 2012 (2,2'-Bipyridyl)-3,3'-diol in Nafion: Stabilization of Unusual Ground and Excited States *J. Phys. Chem. B* **116** 5302
43. Satpathi S, Gavvala K and Hazra P 2015 Fluorescence Up-Conversion Studies of [2,2'-Bipyridyl]-3,3'-diol in Octyl- $\beta$ -D-glucoside and Other Micellar Aggregates *J. Phys. Chem. A* **119** 12715
44. De D and Datta A 2013 Unique Effects of Aerosol OT Lamellar Structures on the Dynamics of Guest Molecules *Langmuir* **29** 7709
45. Mandal S, Ghosh S, Banerjee C, Kuchlyan J and Sarkar N 2013 Roles of Viscosity, Polarity, and Hydrogen-Bonding Ability of a Pyrrolidinium Ionic Liquid and Its Binary Mixtures in the Photophysics and Rotational Dynamics of the Potent Excited-State Intramolecular Proton-Transfer Probe 2,2'-Bipyridine-3,3'-diol *J. Phys. Chem. B* **117** 6789
46. Nag T N, Das T, Mondal S, Maity A and Purkayastha P 2015 Promoting the "Water-Wire" Mechanism of Double Proton Transfer in [2,2'-Bipyridyl]-3,3'-diol by Porous Gold Nanoparticles *Phys. Chem. Chem. Phys.* **17** 6572
47. Ghosh P, Maity A, Das T, Mondal S and Purkayastha P 2013 [2,2'-Bipyridyl]-3,3'-diol in Lipid Vesicles: Slowed Down Dynamics of Proton Transfer *Soft Matter* **9** 8512
48. Banik D, Roy A, Kundu N and Sarkar N 2016 Modulation of the Excited-State Dynamics of 2,2'-Bipyridine-3,3'-diol in Crown Ethers: A Possible Way To Control the Morphology of a Glycine Fibril through Fluorescence Lifetime Imaging Microscopy *J. Phys. Chem. B* **120** 11247
49. Kolthoff I M, Chantooni M K and Wang W J 1983 Protonation and Hydronium Complexation Stability Constants of Several Crown Ethers in Acetonitrile *Anal. Chem.* **55** 1202
50. Behr JP, Dumas P and Moras D 1982 The  $H_3O^+$  Cation: Molecular Structure of an Oxonium-Macrocyclic Polyether Complex *J. Am. Chem. Soc.* **104** 4540
51. Adler-Abramovich L, Vaks L, Carny O, Trudler D, Magno A, Caffisch A, et al. 2012 Phenylalanine Assembly into Toxic Fibrils Suggests Amyloid Etiology in Phenylketonuria *Nat. Chem. Biol.* **8** 701
52. Nandi S, Pyne A, Ghosh M, Banerjee P, Ghosh B and Sarkar N 2020 Antagonist Effects of L-Phenylalanine and the Enantiomeric Mixture Containing D-Phenylalanine on Phospholipid Vesicle Membrane *Langmuir* **36** 2459
53. Perween S, Chandanshive B, Kotamarthi H C and Khushalani D 2013 Single Amino Acid based Self-Assembled Structure *Soft Matter* **9** 10141
54. Lindgren M, Sorgjerd K and Hammarstrom P 2005 Detection and characterization of aggregates, prefibrillar amyloidogenic oligomers, and protofibrils using fluorescence spectroscopy *Biophys. J.* **88** 4200
55. Biancalana M and Koide S 2010 Molecular Mechanism of Thioflavin-T Binding to Amyloid Fibrils *Biochim. Biophys. Acta* **180** 1405
56. Sulatskaya A I, Lavysh A V, Maskevich A A, Kuznetsova I M and Turoverov K K 2017 Thioflavin T fluoresces as excimer in highly concentrated aqueous solutions and as monomer being incorporated in amyloid fibrils *Sci. Rep.* **7** 2146
57. Nandi S, Kundu S, Pyne A and Sarkar N 2020 Spectroscopic investigation on alteration of dynamic properties of lipid membrane in presence of Gamma-Aminobutyric Acid (GABA) *J. Mol. Liq.* **297** 111877
58. Becker W 2012 Fluorescence lifetime imaging - techniques and applications *J. Microsc.* **247** 119
59. Lindgren M, Sorgjerd K and Hammarstrom, P 2005 Detection and Characterization of Aggregates, Prefibrillar Amyloidogenic Oligomers, and Protofibrils using Fluorescence Spectroscopy *Biophys. J.* **88** 4200
60. Biancalana M and Koide S 2010 Molecular Mechanism of Thioflavin-T Binding to Amyloid Fibrils *Biochim. Biophys. Acta* **1804** 1405
61. Lindberg D J, Wranne M S, Gilbert Gatty M, Westerlund F and Esbjörner E K 2015 Steady-State and Time-Resolved Thioflavin-T Fluorescence can Report on Morphological Differences in Amyloid Fibrils Formed by A $\beta$  (1-40) and A $\beta$  (1-42) *Biochem. Biophys. Res. Commun.* **458** 418
62. Maskevich A A, Stsiapura V I, Kuzmitsky V A, Kuznetsova I M, Povarova O I, Uversky V N and Turoverov K K 2007 Spectral Properties of Thioflavin T in Solvents with Different Dielectric Properties and in a Fibril-Incorporated Form *J. Proteome Res.* **6** 1392
63. Stsiapura V I, Maskevich A A, Kuzmitsky V A, Turoverov K K and Kuznetsova I M 2007 Computational Study of Thioflavin T Torsional Relaxation in the Excited State *J. Phys. Chem. A* **111** 4829
64. Lisa-Maria N, Weber J, Pearson C M, Do D T, Gorka F, Lyu G, et al. 2020 A Comparative Photophysical Study of Structural Modifications of Thioflavin T-Inspired Fluorophores *J. Phys. Chem. Lett.* **11** 8406
65. Nandi S, Mukhopadhyay A, Nani P K, Bera N, Hazra R, Chatterjee J and Sarkar N 2022 Amyloids Formed by Nonaromatic Amino Acid Methionine and Its Cross with Phenylalanine Significantly Affects Phospholipid Vesicle Membrane: An Insight into Hypermethionemia Disorder *Langmuir* **38** 8252
66. Nandi S, Pyne A, Layek S, Arora C and Sarkar N 2021 The Dietary Nutrient Trimethylamine N-Oxide Affects the Phospholipid Vesicle Membrane: Probable Route to Adverse Intake *J. Phys. Chem. Lett.* **12** 12411
67. Nandi S, Ghosh B, Ghosh M, Layek S, Nandi P K and Sarkar N 2021 Phenylalanine Interacts with Oleic Acid-Based Vesicle Membrane. Understanding the Molecular Role of Fibril-Vesicle Interaction under the Context of Phenylketonuria *J. Phys. Chem. B* **125** 9776
68. Nandi S, Layek S, Nandi P K, Bera N, Hazra R and Sarkar N 2021 Self-assembly of Artificial Sweetener Aspartame Adversely Affects Phospholipid Membranes: Plausible Reason For its Deleterious Effects *Chem. Commun.* **57** 10532